Kinetics of Electrode Reactions on (110) Single-Crystalline Nickel Electrodes in Nickel Sulfamate Using a Multipulse Current Measurement

M. Saitou* and R. Hashiguchi

Department of Mechanical Systems Engineering, University of the Ryukyus, 1 Senbaru Nishihara-cho, Okinawa 903-0213, Japan

Received: March 31, 2003; In Final Form: May 18, 2003

A method is described for the study of the kinetics of electrode reactions on the basis of analytical solutions of three transient electrochemical processes comprising the diffusion of ions in electrolyte, charge-transfer reactions, and a charging process of an electrochemical double layer. Multipulse currents are applied to a working electrode of (110) single-crystalline nickel in nickel sulfamate, and the potentials between the working and counter electrodes are recorded. The measured potential−time curves well agree with those predicted by the analytical solution. The kinetic constant, exchange current density, and double-layer capacitance characterizing the kinetics of the electrode reactions are determined from the measured potential−time curves using the analytical solution.

Introduction

There have been many attempts to apply galvanostatic pulse function methods[1−4] to the study of kinetic electrode reactions in electrodeposition. These methods have been developed mainly for a single-step electrode reaction but not for multistep electrode reactions with an intermediate accumulation of ions in electrolyte, which is called a homogeneous charge-transfer reaction.[1] The homogeneous charge-transfer reaction takes place at an outer Helmholtz plane.[5] For example, the electrocrystallization of nickel ions occurs mainly in two successive faradic reactions[6,7] of nickel ions Ni^+ such as $Ni^{2+} + e^- \rightarrow Ni^+$ and $Ni^+ + e^- \rightarrow Ni$. These two-step reactions were also supported by our study[8] of the electrocrystallization of nickel ions in nickel sulfamate using electrochemical impedance spectroscopy, which showed that the charge-transfer reactions are homogeneous and the two-step reactions comprise a slow reaction, $Ni^{2+} + e^- \rightarrow Ni^+$, and a fast reaction, $Ni^+ + e^- \rightarrow Ni$.

In this study, the kinetic electrode reactions of nickel ions in nickel sulfamate that have been used for electroforming will be reported on the basis of analysis of three transient processes comprising the diffusion of ions in electrolyte, charge-transfer reactions, and a charging process of the electrochemical double layer. Fundamental parameters that describe the transient behaviors of electrode reactions are determined from potential−time curves measured after the application of square-wave multipulse currents. The small current imposed between working and counter electrodes causes a concentration wave in electrolyte and a charging process of the electrochemical double layer. The concentration wave defined as a concentration of ions deviated from the thermal equilibrium, which is small enough to be treated as a perturbation, is governed by the Fick's diffusion equation.[9] Ni^{2+} ions arriving at the outer Helmholtz plane are involved in the two successive faradaic reactions mentioned above.

In this study, some linearization treatments of nonlinear terms in governing equations are made to derive analytical solutions for the potential−time function, which limits the potential between working and counter electrodes to a few millivolts and under.[10] As a result result, the amplitude of the applied current becomes much smaller than an order of milliampere. Moreover the current on-time should be within an order of millisecond to attain an appropriate accuracy of the solutions.

In galvanostatic pulse current methods, a single or a double current step has been generally applied to the electrochemical cell and the measured potential−time curves obviously depend on the current on-time. Unfortunately, there have been no reports about the measurement of kinetic parameters taking into account three kinetic processes such as the diffusion of ions in electrolyte, charge-transfer reactions, and a charging process of the electrochemical double layer. To avoid the dependence of the measured potential−time curve on the current on-time, multipulse current measurements and analytical treatments are developed in this study. In addition, the multipulse current measurements for the kinetic electrode reactions have not been reported before.

The purposes of this paper are to propose an analytical solution for the kinetic electrode reactions comprising the diffusion of ions in electrolyte, charge-transfer reactions, and a charging process of the electrochemical double layer and to present the kinetic constant, exchange current density, and double-layer capacitance from the multipulse current measurement using the analytical solution.

Experimental Setup

The experimental procedure for the multistep current measurement was as follows: Single-crystalline nickel disks of 12.0 mm in diameter and 1.0 mm in thickness used for working electrodes were prepared to avoid the effect of grain boundaries[11] on the potential−time curves, which had a high purity of 99.999 wt % and the surface orientation (110) determined to an accuracy of 2.0°. The (110) surfaces were polished using 5, 1, and 0.1 μm diamond powder pastes and finally electrochemically etched in a $H_2SO_4-C_3H_5(OH)_3$ (glycerin)$-H_2O$ solution. The average root-mean-square (rms) roughness of the polished surfaces was about 2.3 nm, which was determined from the images observed

* To whom correspondence should be addressed. Telephone number: +81-98-895-8635. Fax number: +81-98-895-8707. E-mail address: saitou@tec.u-ryukyu.ac.jp.

10.1021/jp0348326 CCC: $25.00 © 2003 American Chemical Society
Published on Web 07/19/2003

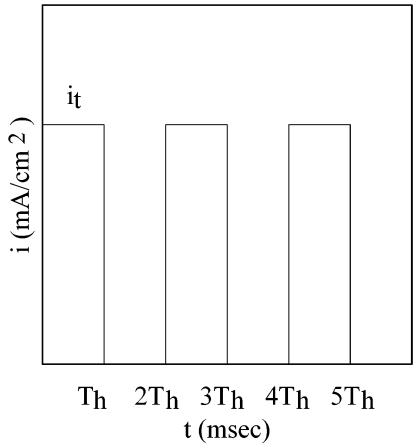

Figure 1. A schematic illustration of multipulse currents applied between the working and counter electrodes. The current density i_t passes through the electrochemical cell during the current on-time T_h. It is noted that the current on-time is equal to the current off-time.

by atomic force microscopy. The surfaces roughness[12] is so small that the effect of surface roughness on the faradic measurements can be ignored. In the case of a slow growth rate, 0.2 monolayer/s, epitaxial nickel thin films are reported to be grown on single-crystalline nickel substrates.[13] Hence in this study, we will have the epitaxial nickel thin films grown on the single-crystalline nickel electrodes because of lower current densities. Polycrystalline nickel sheets of 68 mm long, 60 mm wide, and 0.05 mm thick were prepared for the counter electrodes and polished using abrasive sheets of #800. The area of the counter electrode was 52 times as large as that of the working electrode. Hence, we can ignore the resistance and capacitance in series of the counter electrode in electrolyte compared with those of the single-crystalline nickel electrodes.

Those electrodes cleaned by a wet process were located parallel in a still cell containing (M/L) nickel sulfamate (0.93 or 1.86), nickel chloride (0.0386), and boric acid (0.647). The electrochemical cell was maintained at pH 4 and at a temperature of 300 K. The multipulse currents were supplied by a pulse current generator. The peak amplitude of the current density applied between the electrodes was small, in a range of 0.0217−0.0867 mA/cm^2, which were chosen to fulfill a condition that the measured potentials should be less than a few millivolts. A schematic representation of the square multipulse wave currents is shown in Figure 1. The current on-time, T_h, equal to the current off-time was chosen within a range of 2−8 ms. A digital oscilloscope measured the potential between the working and counter electrodes. A personal computer connected to the digital oscilloscope through a GP−IB bus recorded the potential−time curves.

Analysis of Potential−Time Curves

It has been reported that the electrode reactions on (110) single-crystalline nickel disks in nickel sulfamate are a homogeneous charge-transfer reaction.[8] Hence the boundary condition for the homogeneous charge-transfer reaction is given at an outer Helmholtz plane of $x = 0$ in the x-coordinate normal to the nickel electrode. The reaction

$$Ni^{2+} + e^- \xrightarrow{k} Ni^+$$

takes place at the outer Helmholtz plane where k is the rate constant. The diffusion equation and boundary condition in one dimension for the homogeneous charge-transfer reaction are

$$\frac{\partial \Delta c}{\partial t} = D\frac{\partial^2 \Delta c}{\partial x^2} \tag{1}$$

$$k(c^* - \Delta c) = -D\frac{\partial \Delta c}{\partial x} \quad \text{at} \quad x = 0 \tag{2}$$

where $\Delta c = c^* - c$ is a small concentration change of Ni^{2+} ions caused by multistep currents, c^* is the thermal equilibrium concentration of Ni^{2+} ions in electrolyte, c is the transient concentration of Ni^{2+} ions, and D is the diffusion coefficient. Equation 2 indicates that the flux of Ni^{2+} ions transported by diffusion is equal to the number of Ni^+ ions reduced from Ni^{2+} ions. Equation 1 can be solved under the boundary condition (eq 2) using the Laplace transformation such as $\int_0^\infty e^{-pt}\,\Delta c\,dt$. The solution of eq 1 is

$$\Delta \bar{c} = M \exp\left(-\sqrt{\frac{p}{D}}x\right) \tag{3}$$

where $\Delta \bar{c}$ indicates the concentration in the Laplace space and M is an integral constant, which is determined from the equation that is transformed eq 2 into the Laplace space as follows:

$$M = \Delta \bar{c}|_{x=0} = \frac{kc^*}{p(\sqrt{pD} + k)} \tag{4}$$

Here let us consider a square-wave current pulse at a time t where $2mT_h < t < (2m + 1)T_h$ where T_h is the on-time and m is an integer. The square-wave current step i applied between the working and counter electrodes at the time $2mT_h < t < (2m + 1)T_h$ is given by

$$i = i_t[U(t) - U(t - T_h) + U(t - 2T_h) - \ldots - U(t - (2m + 1)T_h)] \tag{5}$$

and

$$U(t) = \begin{Bmatrix} 1 & \text{for} & t \geq 0 \\ 0 & \text{for} & t < 0 \end{Bmatrix}$$

where i_t is the peak current density as shown in Figure 1. We set the current on-time equal to the current off-time. This makes it easier to derive solutions of the problem in this study. Equation 5 is also transformed into the Laplace space as

$$\bar{\imath} = \frac{i_t}{p}\frac{1 - e^{-2(m+1)pT_h}}{1 + e^{-pT_h}} \tag{6}$$

where $\bar{\imath}$ indicates the current transformed into the Laplace space. The current i can be divided into two elements, the faradaic current density, i_f, and the capacity current density, i_c, that passed through the electrochemical double layer,

$$i = i_c + i_f \tag{7}$$

The faradaic current density[1,3] related to the charge-transfer reaction $Ni^+ + e^- \rightarrow Ni$ is

$$i_f = i_o\left[\frac{c_O}{c_O^o}\exp\left(-\frac{\alpha FE_c}{RT}\right) - \frac{c_R}{c_R^o}\exp\left(-\frac{(1-\alpha)FE_c}{RT}\right)\right] \cong i_o\left(\frac{c_O}{c_O^o} - \frac{c_R}{c_R^o} - \frac{F}{RT}E_c\right) \tag{8}$$

where α is the transfer coefficient for the process, c_O and c_R

are the concentrations of Ni^+ and Ni, c_O^o and c_R^o are the thermal equilibrium concentrations of Ni^+ and Ni, respectively, i_o is the exchange current density, and E_c is the electrode potential that occurs during the charge-transfer reaction. It is noted that eq 8 is linearized under a reasonable approximation of E_c not exceeding a few millivolts. On the other hand, the capacitance current density[3] is

$$i_c = -C\frac{dE}{dt} \tag{9}$$

where C is the electrochemical double-layer capacitance. The potential of the double-layer capacitance E is equal to the sum of E_c and the diffusion potential E_d,

$$E = E_c + E_d \tag{10}$$

For $\Delta c/c^* \ll 1$, the diffusion potential is linearized as

$$E_d = \frac{RT}{F}\ln\frac{c}{c^*} \approx \frac{RT\Delta c}{Fc^*} \tag{11}$$

Substituting eqs 8 and 9 into eq 7 and again substituting eqs 10 and 11 into the result, we have the following equation transformed into the Laplace space,

$$\bar{E} = -\frac{\bar{\imath}}{cp\left(p+\frac{Fi_o}{CRT}\right)} + \frac{i_o k}{C\sqrt{D}p\left(p+\frac{Fi_o}{CRT}\right)\left(\sqrt{p}+\frac{k}{\sqrt{D}}\right)} \tag{12}$$

Here we assume that $c_O^o = c_R^o$ and $c_O = c_R$, which are often used in analysis of electrode reactions. To obtain a solution in the real space, the inverse Laplace transform is applied to eq 12, for example,

$$\frac{\bar{\imath}}{p\left(p+\frac{Fi_o}{CRT}\right)} \rightarrow \frac{RTi_t}{Fi_o}\left(1-\frac{e^{mFi_oT_h/(CRT)}-e^{-2mFi_oT_h/(CRT)}}{1+e^{mFi_oT_h/(CRT)}}e^{-Fi_ot/(CRT)}\right) \tag{13}$$

Here eq 6 is substituted into the first term in eq 13. Thus the solution of the potential−time function in the real space is

$$E = -\frac{RTi_t}{Fi_o}\left(1-\frac{e^{mFi_oT_h/(CRT)}-e^{-2mFi_oT_h/(CRT)}}{1+e^{mFi_oT_h/(CRT)}}e^{-Fi_ot/(CRT)}\right) + \frac{2RTk}{F\sqrt{\pi D}}\sqrt{t} - \frac{RTk^2}{FD}\int_0^t e^{(k^2/D)\theta}\,\mathrm{erfc}\left(k\sqrt{\frac{\theta}{D}}\right)d\theta - \frac{RTk}{F\sqrt{D}}\int_0^t e^{-(Fi_o/(CRT))(t-\theta)}\left[\frac{1}{\sqrt{\pi\theta}} - \frac{k}{\sqrt{D}}e^{(k^2/D)\theta}\,\mathrm{erfc}\left(k\sqrt{\frac{\theta}{D}}\right)\right]d\theta \tag{14}$$

where erfc(...) is the complementary error function and the transformation $t - 2mT_h \rightarrow t$ is used. The third term on the right-hand side in eq 14 can be expanded in a power series of t^n where $n \geq 3/2$. Hence for $t \ll 1$, we can ignore the third term in comparison with the first and second terms. The fourth term on the right-hand side in eq 14 can also be ignored owing to $\exp(-Fi_ot/(CRT)) \ll 1$ for typical values of $t \cong 10^{-3}$ sec, $RT/F = 25.7 \times 10^{-3}$ V, $i_o \cong 1 \times 10^{-3}$ mA/cm^2, and $C \approx 1$ μF at room temperature. Consequently, for the milisecond order and $mT_h \gg 10^2$, eq 14 is simplified and can be rewritten as

$$E = -\frac{RTi_t}{Fi_o}(1-e^{-Fi_ot/(CRT)}) + \frac{2RTk}{F\sqrt{\pi D}}\sqrt{t} \tag{15}$$

This is a proposed potential−time function in this study. Figure 2 shows a typical representation of eq 15. Equation 15 well explains physical responses of ions to the applied pulse current. The exponential term on the right-hand side in eq 15 is related to a charging process of the electrochemical double layer. The square root of time represents the movements of the ions by diffusion.

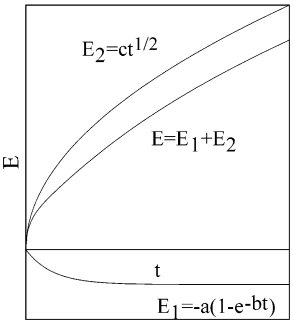

Figure 2. Potential−time curves presented in eq 15 where $a = RTi_t/(Fi_o)$, $b = Fi_o/(CRT)$, and $c = 2RTk/(F\sqrt{\pi D})$.

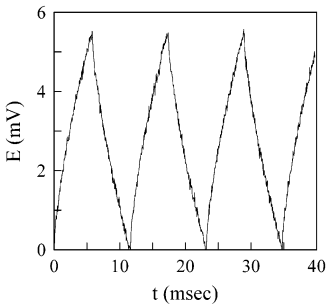

Figure 3. Typical potential−time curves for $i_t = 0.0867$ mA/cm^2, $T_h = 6$ ms, $c^* = 1.86$ M/L (a concentration of nickel sulfamate), and $2mT_h = 3.6 \times 10^2$ s.

Results and Discussion

In this study, many potential−time curves were measured for two nickel sulfamate concentrations and four current on-times. A typical plot of the potential−time curve for $i_t = 0.043$ mA/cm^2, $T_h = 6$ ms, $c^* = 1.86$ M/L (a concentration of nickel sulfamate), and $2mT_h = 3.6 \times 10^2$ s is shown in Figure 3. The potential rises at a slow rate and is delayed in response to the input current. As shown in Figure 3, all of the potential−time curves have the same response to the input currents, which indicates the independence of the potential−time curve on the number of the applied current pulses, m.

Figure 4 shows a plot of the potential−time curves for the four different current on-times at $2mT_h = 3.6 \times 10^2$ s. It can be seen that the four curves during the current on-time collapse on a single curve. Equation 14 indicates that the potential−time curve depends on the current on-time T_h. For a large value of m, eq 14 approaches eq 15, that is, the potential−time curve is independent of the current on-time T, which is supported by Figure 4.

Let us present how to derive the fundamental parameters describing the kinetic electrode reactions from the measured potential−time curves. First, the slopes of $t^{1/2}$ are determined

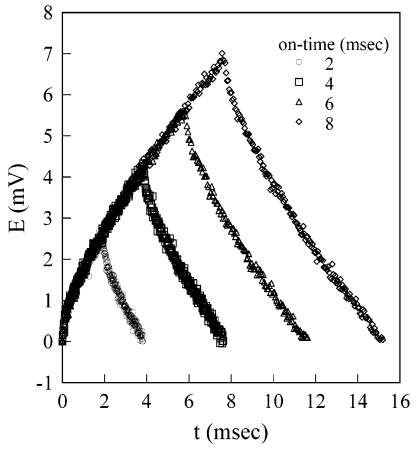

Figure 4. Potential−time curves at four different current on-times of 2, 4, 6, and 8 ms for $i_t = 0.0867$ mA/cm^2, $c^* = 1.86$ M/L, and $2mT_h = 3.6 \times 10^2$ s. These response curves are chosen from the recorded potential−time curves within a time range of $2mT_h = 3.6 \times 10^2$ to $(2m + 1)T_h = 3.6 \times 10^2 + T_h$. The four curves during the current on-time collapse on one curve, which obeys the predictions by eqs 14 and 15.

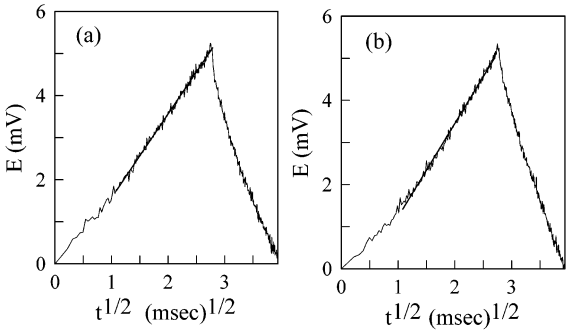

Figure 5. Plots of the potential vs $t^{1/2}$ at $T_h = 8$ ms: (a) $c^* = 0.93$ M/L; (b) $c^* = 1.86$ M/L. The values of the straight lines fitted to the data are used for determination of the plot E_1 in Figure 2.

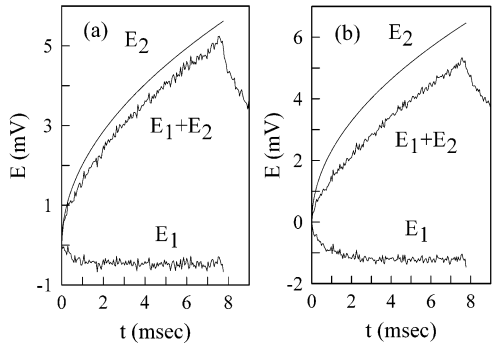

Figure 6. Plots of E_1 and E_2 determined from the measured potential−time curves $E_1 + E_2$. Panels a and b correspond to Figure 5, panels a and b, respectively.

from the plots of E vs $t^{1/2}$ in Figure 5. Then subtracting the calculated values of the potential$-t^{1/2}$ curve from the measured values of the potential−time curve, we have an exponential-type curve that corresponds to the second term on the right-hand side in eq 15. Figure 6 shows that the measured potential−time curve is divided into two curves, as well as depicted in Figure 2. Certainly the curve E_1 in Figure 6 appears to be an exponential-type function that has a saturated value. Because the exponential-type curves saturate at about 2 ms, we mainly choose the potential−time curve at a current on-time of 8 ms to analyze. In the same way, all of the plots of the measured

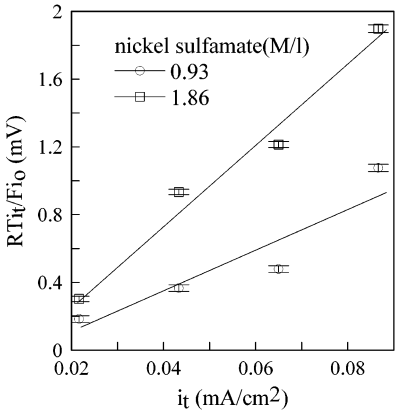

Figure 7. A plot of $RTi_t/(Fi_o)$ vs i_t for two nickel sulfamate concentrations at $T_h = 8$ ms.

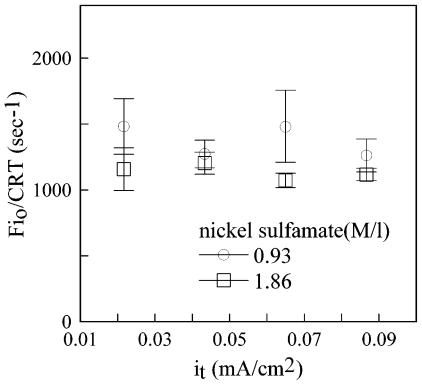

Figure 8. A plot of $Fi_o/(CRT)$ vs i_t for two nickel sulfamate concentrations at $T_h = 8$ ms.

potential−time curves can be divided into the two parts. Thus the potential−time function represented by eq 15 is justified. The three constants in eq 15, $RTi_t/(Fi_o)$, $Fi_o/(CRT)$, and $2RTk/(F\sqrt{\pi D})$, can be determined from Figure 6, and the results are shown in Figures 7, 8, and 9.

Figure 7 is a plot of $RTi_t/(Fi_o)$ vs i_t for two nickel sulfamate concentrations, which indicates that $RTi_t/(Fi_o)$ is linearly proportional to i_t. This enables us to obtain the exchange current density i_o from their slopes. The average exchange current densities for the nickel sulfamate concentrations of 0.93 and 1.86 M/L are determined as 2.0 ± 0.05 and 1.1 ± 0.2 mA/cm^2, respectively.

Figure 8 shows a plot of $Fi_t/(CRT)$ vs i_t for two nickel sulfamate concentrations. The values of $Fi_t/(CRT)$ are almost independent of i_t, and the capacitance of the electrochemical double layer is easily determined. The average double-layer capacitances for the nickel sulfamate concentrations of 0.93 and 1.86 M/L are determined as 63.2 ± 7.0 and 37.6 ± 2.0 μF, respectively.

Figure 9 shows that $k/\sqrt{D}$ is linearly proportional to i_t. The boundary condition eq 2 indicates that

$$k(c^* - \Delta c) = i_f = i_t - i_c \quad \text{at} \quad x = 0 \tag{16}$$

For $\Delta c/c^* \ll 1$ and $i_c \ll i_t$, eq 16 implies that $k \propto i_t$, which also indicates that the small capacitance of the double layer in this case results in a short charging time. In fact, the charging time is estimated at about 2 ms from Figure 6.

Thus, we have the parameters that describe the electrode reaction and can verify the validity of the approximations used in the analysis; for example, $Fi_o/(RTC) > 1 \times 10^4$. However,

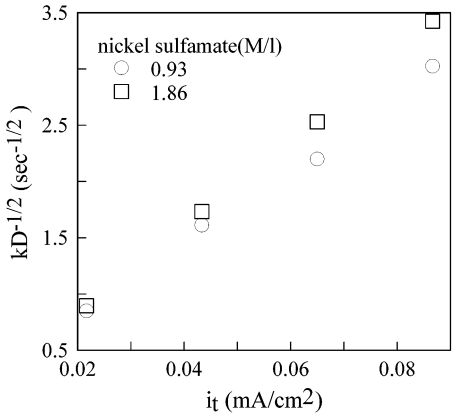

Figure 9. A plot of $k/\sqrt{D}$ vs i_t for two nickel sulfamate concentrations at $T_h = 8$ ms.

there have been no reports about the kinetic parameters measured in nickel sulfamate. The exchange current density for aqueous sulfate solutions[14] was reported. In further studies, comparison between the measured values in this study and those in different studies will be required.

Conclusions

(1) A method is proposed for the study of the kinetics of the electrode reactions using the multipulse current measurement. (2) The analytical solutions for three transient processes comprising the diffusion of ions in electrolyte, charge-transfer reactions, and a charging process of the electrochemical double layer are derived. (3) The measured potential−time curves for (110) single-crystalline nickel disks in nickel sulfamate well agree with those predicted by the analytical solution. (4) The kinetic constant, exchange current density, and double-layer capacitance characterizing the kinetics of the charge-transfer reactions are determined from the measured potential−time curves using the proposed analytical solution.

Acknowledgment. The first author would like to thank Mr. Hideki Higa in the university of the Ryukyus for the experimental preparations.

References and Notes

(1) Vetter, K. J. *Electrochemical Kinetics*; Academic Press: New York, 1967; pp 413−432.
(2) Bockris, J. O'M.; Reddy, A. K. N.; G-Aldeco, M. *Modern Electrochemistry 2A*; Kluwer Academic: New York, 2000; pp1409−1414.
(3) Berzins, T.; Delhay, P. *J. Am. Chem. Soc.* **1955**, *77*, 6448.
(4) Matsuda, H.; Oka, S.; Delhay, P. *J. Am. Chem. Soc.*, **1959**, *81*, 5077.
(5) Pandey, P. K.; Sahu, S. N.; Chandra, S. *Handbook of Semiconductor electrodeposition*; Marcel Dekker Inc.: New York, 1996; pp 10−14.
(6) Holm, M.; O'Keefe, T. J. *J. Appl. Electrochem.* **2000**, *30*, 1125.
(7) Lachenwitzer, A.; Magnussen, O. M. *J. Phys. Chem. B* **2000**, *104*, 7414.
(8) Saitou, M.; Hamaguchi, K.; Inoue, K. *J. Phys. Chem. B* **2002**, *106*, 12253.
(9) Crank, J. *The Mathematics of Diffusion*; Clarendon Press: Oxford, U.K., 1975.
(10) Nagy, Z.; Hung, N. C.; Liddell, K. C.; Minkoff,; M.; Leaf, G. K. *J. Electroanal. Chem.* **1997**, *421*, 33.
(11) Bisquert, J. *Phys. Chem. Chem. Phys.* **2000**, *2*, 4185.
(12) Larsen, A. E.; Grier, D. G. *Phys. Rev. E* **1995**, *52*, R2161.
(13) Saitou, M.; Hamaguchi, K.; Oshikawa, W. *J. Electrochem. Soc.* **2003**, *150*, C99.
(14) Mohanty, U. S.; Tripathy, B. C.; Singh, P.; Das, S. C. *J. Appl. Electrochem.* **2001**, *31*, 969.